Ionic fragmentation of a CH_4 molecule induced by 10-keV electrons: Kinetic-energy-release distributions and dissociation mechanisms

Raj Singh, Pragya Bhatt, Namita Yadav, and R. Shanker*
Atomic Physics Laboratory, Department of Physics, Banaras Hindu University, Varanasi-221005, India
(Received 9 April 2013; published 25 June 2013)

The dynamics of ionic fragmentation of CH_4 molecules under impact of 10-keV electrons has been studied. The technique of recoil ion momentum spectroscopy is employed to obtain information about the kinetic energy release and the dissociation mechanisms of different pathways arising from the fragmentation of a CH_4 dication. The results show that there are altogether eight dissociation pathways that arise from the complete and the incomplete Coulomb explosions of the $CH_4{}^{2+}$ molecular ions. The kinetic energy release for these pathways is compared with earlier data from the literature for the impact of different charged particles, photons, and their impact energies. The present results indicate that mostly the lower electronic states of $CH_4{}^{2+}$ are involved for the observed dissociation channels. Also, the dissociation mechanisms associated with these channels are suggested and discussed. Further, we have also estimated the relative ion intensities of different channels of fragmentation of CH_4 dication produced under impact of considered energy of electrons.

DOI: 10.1103/PhysRevA.87.062706 PACS number(s): 34.80.Gs, 34.80.Ht

I. INTRODUCTION

The fragmentation of multiply charged molecular ions is a very active area of research in recent years [1–4]. The study of fragmentation dynamics of molecular ions not only sheds light on the processes taking place in reaction processes of fundamental and applied sciences but also it is very important to identify and understand the nature of electronic states involved in the fragmentation reaction of the precursor ion. Measurements of the kinetic-energy-release distributions (KERDs) of fragment species provide a stringent testing ground for different theoretical models [5,6]. Further, such studies find wide applications in several areas of science and technology, for example, in plasma physics, atmospheric physics, astrophysics, radiation physics, and in chemistry [7–10]. CH_4 is one of the smallest hydrocarbon molecules that has a tetrahedral geometry in its ground state. This molecule is found in the earth's atmosphere and forms a very important constituent of the upper planetary atmosphere [11,12]. It is also a very potent greenhouse gas after carbon dioxide [13]. In particular, the fragmentation of CH_4 induced by galactic cosmic rays (photons, electrons, and ions) produces highly reactive radicals, which not only form complex molecules but also change their concentrations due to chemical coupling between ionic and neutral species [14].

Several studies have been devoted in the past to fragmentation of CH_4 with the interaction of protons, highly charged ions, lasers, synchrotron radiation, and electrons ([15–19] and references therein). In these studies most of the work has involved the determination of total and/or partial ionization cross sections; only few of them are devoted to the measurements of kinetic energy release (KER) and the associated dissociation mechanism for a given dissociation channel. The determination of KER of a dissociation channel arising from a molecular ion is considered to be a very efficient tool to obtain useful information about its relevant electronic states and potential energy surfaces (PESs). Further, some efforts have been made on the theoretical calculations for appearance potential of specific ionic fragments, energy-dependent cross sections of different dissociation channels, and for electronic structure of molecular ions or of excited molecules [20–22]. The advent of position-sensitive detectors and fast electronics has made the measurements possible to determine the position of an ion (x,y) and the corresponding time of flight (t) from its birth place to the detector in a collision event. Such measurements enable one to calculate the momentum vectors of the fragment ions produced in the given collision reaction. The momentum vectors thus obtained yield precise information on the KERD of a dissociation channel [23–25]. From the ion impact, Ben-Itzhak *et al.* [26] and Werner *et al.* [27] have measured the KERD for a number of dissociation channels arising from fragmentation of a multiply charged CH_4 molecule. Recently, Flammini *et al.* [28] and Kukk *et al.* [29] have measured the kinetic energy of the fragment ions arising from the fragmentation of $CH_4{}^{2+}$ using an Auger electron-ion-ion coincidence technique for collisions of CH_4 molecules with 4-keV electrons and with synchrotron radiation, respectively. They have also assigned the dissociation mechanisms for these channels. The ionization of a molecule depends on the energy of the incident projectile. All of the earlier studies have been carried out with relatively low energy of electron impacts; however, the data at intermediate impact energies of electrons are scarce. It was therefore considered worthwhile to study not only the fragmentation dynamics of this molecule under impact of keV electrons but also to see whether there is any signature of trications of the molecule getting formed in such energetic collisions.

In the present work, we have studied the fragmentation dynamics of CH_4 molecules under impact of 10-keV electrons employing the technique of recoil ion momentum spectroscopy. The kinetic energy release for different channels arising from the fragmentation of $CH_4{}^{2+}$ is studied and compared with the data available in the literature for different projectiles and their impact energies. The possible dissociation mechanisms as well as determination of the

*shankerorama@gmail.com

 ©2013 American Physical Society

relative abundances for different ion species arising from the fragmentation of multiply charged CH_4 molecule are presented and discussed.

II. EXPERIMENT SETUP AND DATA ANALYSIS

The present study of fragmentation of CH_4 molecules under 10-keV electron impact has been performed on a recoil ion momentum spectrometer system. The details of the experiment setup and data analysis have been described in our previous publications [23,30]. In brief, a monoenergetic beam of 10-keV electrons was obtained from a commercial electron gun. The beam was made to collide with dilute CH_4 molecules (99.99%) effusing from a hypodermic needle of high aspect ratio (length = 1.2 cm, diameter = 0.01 cm). A Willey-McLaren-type single-stage linear time-of-flight (TOF) mass spectrometer [31] equipped with a position-sensitive detector [32] was used to detect and analyze the mass-to-charge ratio of the fragment ions. The electron beam, the CH_4 gas jet, and the axis of TOF spectrometer were aligned perpendicular to each other. The electrons and positive ions produced from a single collision event in the interaction region were extracted by applying a homogeneous electric field of 266 V/cm. The electrons were detected in pulse counting mode by a channel electron multiplier (CEM) mounted just behind the electron extraction mesh in the opposite direction to that of the ion detector. The electron signals were used as the timing reference for ion arrivals to a dual microchannel plate (MCP) detector. The data was stored in event-by-event mode and analyzed offline by using the Cobold PC software. In order to ensure the full collection efficiency of ions arising from the fragmentation of $CH_4{}^{2+}$, we have performed ion-trajectory calculations using SIMION8.0 code for the present experimental conditions. It was found that all H^+ ions having energy $\leqslant$16 eV and moving in the transverse direction to the electric field are completely detected. In our experiment, the most energetic H^+ ions have kinetic energy peak at 8 $\pm$ 0.5 eV; this check ensures that all the other heavier ions are also fully collected. We note that the dead time of our detector system for two concomitant ions originating from the same collision event is 5 ns.

In order to determine the relative abundance of different fragment ions, the background subtracted ion counts $N(X^+)$ are obtained from the TOF spectrum (see Fig. 1), where $X^+ = CH_4{}^+, CH_3{}^+, CH_2{}^+, CH_2{}^+, C^+, H^+$, and $H_2{}^+$; when these ion counts are divided by the ion counts of $CH_4{}^+$, the relative abundance for the X^+ ion is obtained. The involved errors in the relative abundance are estimated by using the analysis procedures given in Ref. [33]. The overall uncertainties in the data presented here for $CH_4{}^+$, $CH_3{}^+$, $CH_2{}^+$, $CH_2{}^+$, C^+, H^+, and $H_2{}^+$ ions are 1.5%, <2%, 4%, 4%, 5%, 4%, and 6%, respectively.

The TOF (t) and the position (x,y) information of the fragment ions detected in coincidence are used to calculate the momentum vectors $(\mathbf{p}_x,\mathbf{p}_y,\mathbf{p}_z)$ of individual ions using the formulation given in Ref. [23]. The neutral fragments involved in a dissociation channel are not detected in the present experiment; however, their momentum vectors could be estimated from application of the principle of momentum conservation. From the knowledge of momentum vectors of considered fragments, we calculate the KER by summing the kinetic energy of individual ions involved in that channel using the formulation given below,

$$\mathrm{KER} = \sum_i KE_i = \sum_i \frac{p_i^2}{2m_i} \tag{1}$$

Where, KE_i, p_i, and m_i are the kinetic energy, momentum, and mass of ith($i \leqslant 3$) fragment ion, respectively.

The slope and shape of an island obtained from the ion-ion coincidence map (see Fig. 2) provide information about the dissociation mechanism whether it is concerted or sequential [34,35]. In the concerted process, all bonds of the molecule break instantaneously while the stepwise dissociation of the molecule takes place in a sequential manner. There are two type of sequential dissociation; initial charge separation [s(i)] and deferred charge separation [s(d)]. The theoretical value of slopes for these processes can be calculated from the formulation [34–36] as given below: For s(i), the slope of

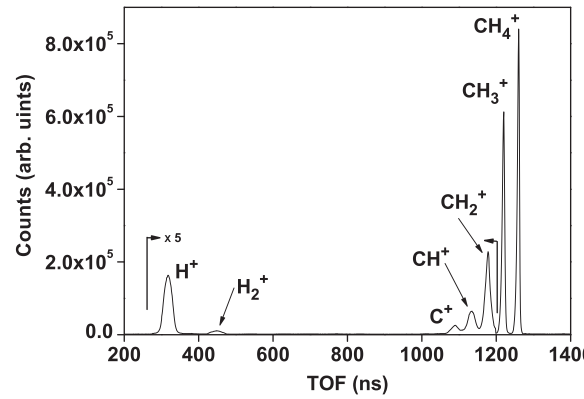

FIG. 1. TOF spectrum of the ions produced from direct and dissociative ionization of a CH_4 molecule by impact of 10-keV electrons.

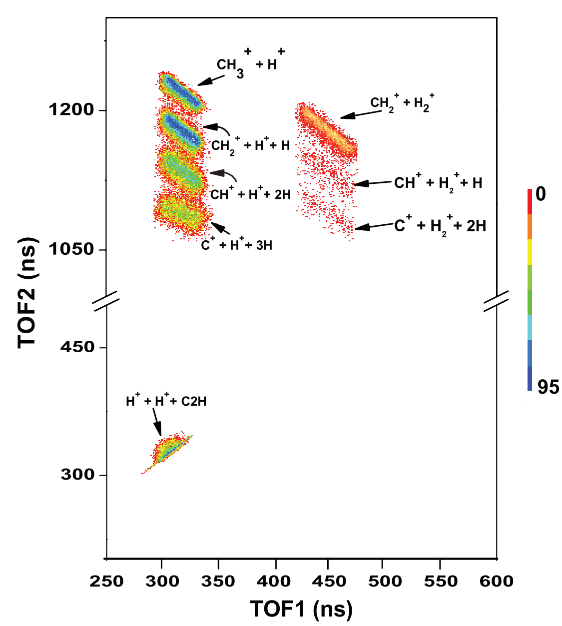

FIG. 2. (Color online) Ion-ion coincidence map resulting from dissociative ionization of $CH_4{}^{2+}$ dication produced in 10-keV electron collisions with CH_4 molecule.

the island is given by

$$\text{slope} = -\left(\frac{q_1}{q_2}\right)\left\{\frac{(m_1+m_3)}{m_1}\right\} \quad \text{or} \quad -\left(\frac{q_1}{q_2}\right)\left\{\frac{m_2}{(m_2+m_3)}\right\}, \tag{2}$$

depending on whether the secondary process gives rise to the lighter or heavier ions, where q_1 and q_2 are the charges on the masses m_1 and m_2 of the first and second fragment ions, respectively and m_3 is the mass of the undetected neutral atom in a dissociation channel. While, for s(d), the slope is given by

$$\text{slope} = -\left(\frac{q_1}{q_2}\right). \tag{3}$$

III. RESULTS AND DISCUSSION

The TOF spectrum produced from the collision of CH_4 molecules with 10-keV electrons is presented in Fig. 1. This spectrum is obtained by performing coincidences between the fragment ions and the correlated electrons originating from the same collision event. The $CH_4{}^+$ ions are found to arise from events of direct ionization of the parent molecule while six other singly charged fragments ($CH_3{}^+$, $CH_2{}^+$, CH^+, C^+, H^+, and $H_2{}^+$) are produced from its dissociative ionization processes. The $CH_4{}^+$ ion exhibits the most intense peak among all the fragment ions in the present experiment. The relative abundance of all the ions relative to the $CH_4{}^+$ ion is listed in Table I. It is generally believed that above a certain value of the impact energy, the relative abundance of the ion species becomes almost impact energy independent; this energy is close to 40 eV for the hydrocarbons [37]. In view of this, we have compared our data for the relative abundance of different fragment ions with those of MeV protons (see Table I), because the MeV protons have the velocities in the same range as those of the keV electrons. It is found from Table I that the relative abundance of the fragment ions ranging from $CH_4{}^+$ to C^+ decreases as the number of missing neutral H atoms increases. The relative abundance for $CH_3{}^+$ is almost the same for all impact energies except for the data of Adamczyk *et al.* [38]; the reason for the large discrepancy with the data of Adamczyk *et al.* [38] may be due to the incomplete collection efficiency of lighter ions (H^+ and $H_2{}^+$) in their experiments. Furthermore, we observe disagreement for the less abundant ions particularly for those which have more than one missing neutral H atoms, for example, $CH_2{}^+$, CH^+, and C^+. The reason for this disagreement is possibly due to the greater contribution to the relative ionic abundance stemming from the dipole nonallowed transitions (Auger-like auto ionization), noting that the possibility of the dipole nonallowed transitions increases with impact energy [39]. Since the light ions (H^+ and $H_2{}^+$) are involved in this fragmentation process, the collection efficiency of the detectors employed to detect these ions in different experiment setups may differ and affect their relative abundances. It is noted that Backx *et al.* [16] have measured the fragment ions arising from the fragmentation of CH_4 under impact of 10-keV electrons, which is shown in column 3 of Table I; they have measured only five ion species, namely, $CH_4{}^+$, $CH_3{}^+$, $CH_2{}^+$, CH^+, and H^+. The reason for the nonobservation of fragment ions C^+ and $H_2{}^+$ in their experiment is not clear; it may be due to the limited statistics of the data in their experiments.

The ion-ion coincidence map is produced from the measurements of two ions in coincidence with electrons originating from the same collision event; it is observed that eight fragmentation channels originate from the dissociation of $CH_4{}^{2+}$ ions (see Fig. 2). The relative intensity for these channels is given in Table II. The relative intensity for some channels reported by Backx *et al.* [16] at our impact energy is also given in Table II. We have also checked the triple-ion coincidences in our data, but we could not find sufficient statistics for any channel arising from the fragmentation of $CH_4{}^{3+}$ molecular ion. In view of this, it is suggested that only single and double ionization of the CH_4 molecule preferentially occur at the considered impact energy. The KERDs and dissociation mechanisms for the above channels are discussed in detail in the following sections.

TABLE I. Comparison of the relative abundance of the ions produced in 10-keV electron impact with CH_4 molecule with the earlier results reported by others.

	Abundance (%)					
	e^- impact				H^+ impact	
Ion species	10 keV (Present)	10 keV[a]	1 keV[b]	1 keV[c]	4 MeV[d]	2.25 MeV[e]
$CH_4{}^+$	100 ± 1.5	100	100	100	100	100
$CH_3{}^+$	85.40 ± 1.7	86	94.7	80.95	84.7	84
$CH_2{}^+$	16.24 ± 0.65	11	13.2	13.1	13.1	9.7
CH^+	9.43 ± 0.38	3.8	4.6	4.3	4.3	3.1
C^+	6.48 ± 0.32		1.4	1.02	1.02	0.6
H^+	17.46 ± 0.70	10.0	6.1	14.47	10.3	
$H_2{}^+$	4.25 ± 0.25		1.1	11.39	0.71	

[a]Reference [16].
[b]Reference [38].
[c]Reference [15].
[d]Reference [26].
[e]Reference [42].

TABLE II. Comparison of the slopes of various islands observed in ion-ion coincidence map obtained from 10-keV electron impact with CH_4 with earlier reported experimental and theoretical results obtained using the formulation from [34–36]; s(i) and s(d) refer to sequential decays with initial charge separation and deferred charge separation, respectively. The relative intensities for various channels obtained from 10-keV electron impact with CH_4 and earlier reported experimental results at 10-keV electron impact with CH_4 are also given.

	Rel. intensity (%)		Slope			
			Theoretical values		Experimental results: e^- impact	
Coincidence channel	Present	10 keV[a]	s(i)	s(d)	Present	4 keV[b]
$CH_3^+ + H^+$	20.68	22.98			-1.00 ± 0.02	-1.03 ± 0.17
$CH_2^+ + H^+ + H$	25.76	32.64	-0.93	-1.0	-0.94 ± 0.04	-1.11 ± 0.18
$CH^+ + H^+ + 2H$	18.40	22.29	-0.87	-1.0	-0.90 ± 0.04	-0.93 ± 0.16
$C^+ + H^+ + 3H$	12.47	14.71	-0.80	-1.0	-0.68 ± 0.06	-0.68 ± 0.15[c]
$H^+ + H^+ + C2H$	15.25					
$CH_2^+ + H_2^+$	6.46	0.32			-1.00 ± 0.02	-1.01 ± 0.17
$CH^+ + H_2^+ + H$	0.63		-0.93	-1.0	-0.97 ± 0.08	
$C^+ + H_2^+ + 2H$	0.36		-0.86	-1.0	-0.80 ± 0.08	

[a]Reference [16].
[b]Reference [28].
[c]It is taken from 238 eV Auger electron-ion-ion coincidence [28].

A. Complete Coulomb fragmentation

The KERD for the channel $CH_3^+ + H^+$ arising from the complete Coulomb fragmentation of CH_4^{2+} precursor ion is shown in Fig. 3(a). The peak of the KERD is found to be at 3.0 ± 0.4 eV. This KERD is compared with those of others at different impact energies and projectiles (see Table III). In order to understand the KERD for this channel, we have taken the energy of the minimum of the PESs for CH_4^{2+}, their dissociation limits, and the KER values from Ref. [28], which are given in Table IV. It is obvious from this table that the states $^3T_1$ and ^1E contribute significantly to the observed KERD, whereas the contribution of the state $^1A_1$ is possibly small. It is found that the upper bound of the FWHM of our KERD for the channel $CH_3^+ + H^+$ shows reasonably good agreement with the KER data of Flammini *et al.* [28], which were obtained from the measurements of 250-eV Auger electron-ion-ion coincidences under impact of 4-keV electrons. However, the peak value of our KERD is found to be smaller than those of proton and the photon impacts [26,40] (see Table III). Flammini *et al.* [28] have also determined the minimum energy structure for different electric energy states of CH_4^{2+} and CH_3^+ and have shown that these states have different geometries than that of the ground state of the parent molecule. Further, it is found from the ion-ion coincidence map (Fig. 2) that slope of the island for the considered channel is -1.0 ± 0.02 and the shape is relatively narrow. This indicates that a two-body fragmentation process is operative in which both fragment ions fly back-to-back to obey the law of momentum conservation.

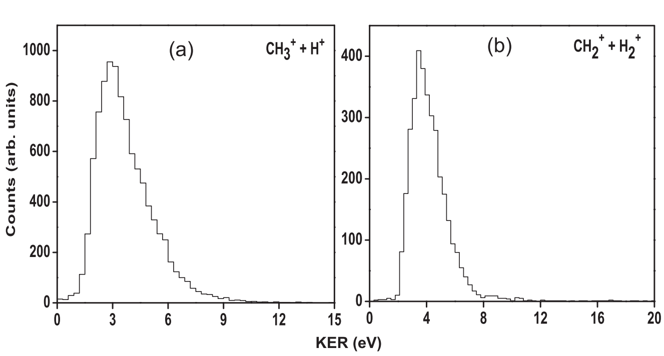

FIG. 3. KER distributions for the complete Coulomb explosion channels: (a) and (b) observed in the dissociation of CH_4^{2+} in 10-keV electron impact with CH_4.

The channel $CH_2^+ + H_2^+$ also arises from the complete Coulomb fragmentation of a CH_4^{2+} dication. The intensity of this channel is quite small in comparison to the above discussed channel. The KERD is shown in Fig. 3(b), which has a peak value at 3.5 ± 0.4 eV. No theoretical data is available for the KER for this channel. Moreover, the KER data from other workers are included in Table III. From the data of 250-eV Auger electron-ion-ion coincidence, Flammini *et al.* [28] have reported the upper bound of KER for this channel. The upper bound of the FWHM of our KERD shows a reasonably good agreement with their data, whereas the KER value from the proton impact [26] underestimates the peak value of our KERD (see Table III). From our ion-ion coincidence map, the slope and shape of the island of this channel are found to be -1.0 ± 0.02 and very narrow, which suggests again the similar conclusions as those drawn for the previous channel. It has been shown theoretically that the H_2^+ is formed via an intramolecular α-elimination mechanism [28]. The formation of H_2^+ due to the rearrangement of the atoms during fragmentation has been also reported in the case of CH_3Cl [41]. The comparison of KER values discussed above shows that the electronic states of CH_4^{2+} as suggested by Flammini *et al.* [28] are most likely involved in our experiments too, which are the lowest electronic state of a CH_4^{2+} dication. Whereas Ben-Itzhak *et al.* [26] from their ion impact data have suggested the involvement of higher electronic states of CH_4^{2+} in their experiments.

TABLE III. Comparison of kinetic energy release in different dissociation channels obtained by impact of 10-keV electrons on CH_4 with the earlier reported experimental results.

	KER (eV)				
	Electron impact		Ion impact		
Dissociation Channel	Present	4 keV[a]	742 keV O^{7+} ions[b]	4 MeV H^+ ions[c]	Photon impact 295 eV[d]
$CH_3^+ + H^+$	3.0 ± 0.4	4.34 ± 0.89	5.0	7.0 ± 0.5	5.75
$CH_2^+ + H^+ + H$	5.0 ± 0.8	4.41 ± 0.90		6.7 ± 0.5	
$CH^+ + H^+ + 2H$	4.7 ± 0.9	4.33 ± 0.89		7.7 ± 0.5	
$C^+ + H^+ + 3H$	6.5 ± 1.0	5.8 ± 1.27		11.9 ± 0.7	
$H^+ + H^+ + C2H$	11.5 ± 2.0				
	4.2 ± 0.8				
$CH_2^+ + H_2^+$	3.5 ± 0.4	5.14 ± 0.71	5.5	7.0 ± 1.0	
$CH^+ + H_2^+ + H$	4.0 ± 1.0				
$C^+ + H_2^+ + 2H$	3.7 ± 1.0				

[a]Reference [28].
[b]Reference [27].
[c]Reference [26].
[d]Reference [40].

B. Incomplete Coulomb fragmentation

We observe six channels ($CH_2^+ + H^+ + H$, $CH^+ + H^+ + 2H$, $C^+ + H^+ + 3H$, $H^+ + H^+ + C2H$, $CH^+ + H_2^+ + H$, and $C^+ + H_2^+ + 2H$) arising from the incomplete Coulomb explosion of the CH_4^{2+} dication. The channel $CH_2^+ + H^+ + H$ is found to be the most intense among all the channels originating either from the complete Coulomb fragmentation or from the incomplete Coulomb fragmentation (see Table II). The KERDs for all channels arising from the incomplete Coulomb fragmentation of the CH_4^{2+} ion are shown in Figs. 4(a)–4(f). The peak value of the KERDs for all the channels are given in Table III. The KER data available in the literature for different projectiles and impact energies are also given in Table III taken from [26–28,40]. It is noted that the KER values taken from [26–28,40] for the channels arising from the incomplete Coulomb fragmentation are the sum of kinetic energies of the individual observed ions; in these data sets, the authors have not considered the contribution of the kinetic energy of neutral fragments present in different channels and have reported the corresponding upper bound of the FWHM of the KERD. The data taken from Ref. [28] is only for 250-eV Auger electron-ion-ion coincidence experiment for impact of 4-keV electrons with CH_4 molecule.

The values of KERD peaks for channels $CH_2^+ + H^+ + H$, $CH^+ + H^+ + 2H$, and $C^+ + H^+ + 3H$ are found at 5.0 ± 0.8 eV, 4.7 ± 0.9 eV, and 6.5 ± 1.0 eV, respectively. No theoretical calculations for KER are presently available in the literature for these channels. If we do not consider the contribution of neutrals to the KERD, we can compare our data with those available from Ref. [28]. The KE peaks for the neutrals of the channels $CH_2^+ + H^+ + H$, $CH^+ + H^+ + 2H$, and $C^+ + H^+ + 3H$ lie at 0.75 eV, 0.60 eV, and 0.90 eV, respectively. On one hand, the comparison of our KER data shows a reasonable agreement with those of Flammini *et al.* [28]. On the other hand, the KER data of proton impact from Ben-Itzhak *et al.* [26] underestimate our KER data. This comparison clearly suggests that the lower electronic states of the CH_4^{2+} molecular ions are preferentially involved in electron impact experiments than those of ion impact (Ben-Itzhak *et al.* [26]). It appears that we possibly excite those states, which are accessed by Flammini *et al.* [28] in their experiment for 250-eV Auger electron-ion-ion coincidence measurements. The slope for the channel $CH_2^+ + H^+ + H$ is found to be −0.94 ± 0.04, which shows reasonably a good agreement with theoretically predicted value for the sequential decay process [s(i)] (see Table II). The Newton diagram for this channel is shown in Fig. 5(a) wherein the peak value of the momentum distribution for H^+ ion is plotted along the x axis and the momentum distributions of the CH_2^+ ion and those of neutral H atom are plotted on the upper and lower half of the x axis, relative to H^+ ion, respectively. The peak of the momentum distributions for the CH_2^+ and that of the neutral H is at about 158° ± 15° and 100° ± 15° respectively. This also suggests that initially CH_4^{2+} dication fragments into CH_3^+ and H^+ ions and in the next step, CH_3^+ dissociates into CH_2^+ and H to balance the momentum of the center of mass of CH_3^+. Flammini *et al.* [28] have observed the similar dissociation process with

TABLE IV. The possible molecular states of CH_4^{2+} dissociating into $CH_3^+ + H^+$ together with the theoretically calculated values of KER [28].

Molecular states	Energy of states (eV)	KER (eV)	Dissociation limit	Dissociation limit value (eV)
$^1A_1$	38.5	6.9	$CH_3^+(^1E') + H^+$	31.6
$^3T_1$	33.8	3.1	$CH_3^+(^3E') + H^+$	30.7
^1E	31.1	4.6	$CH_3^+(^1A'_1) + H^+$	26.5

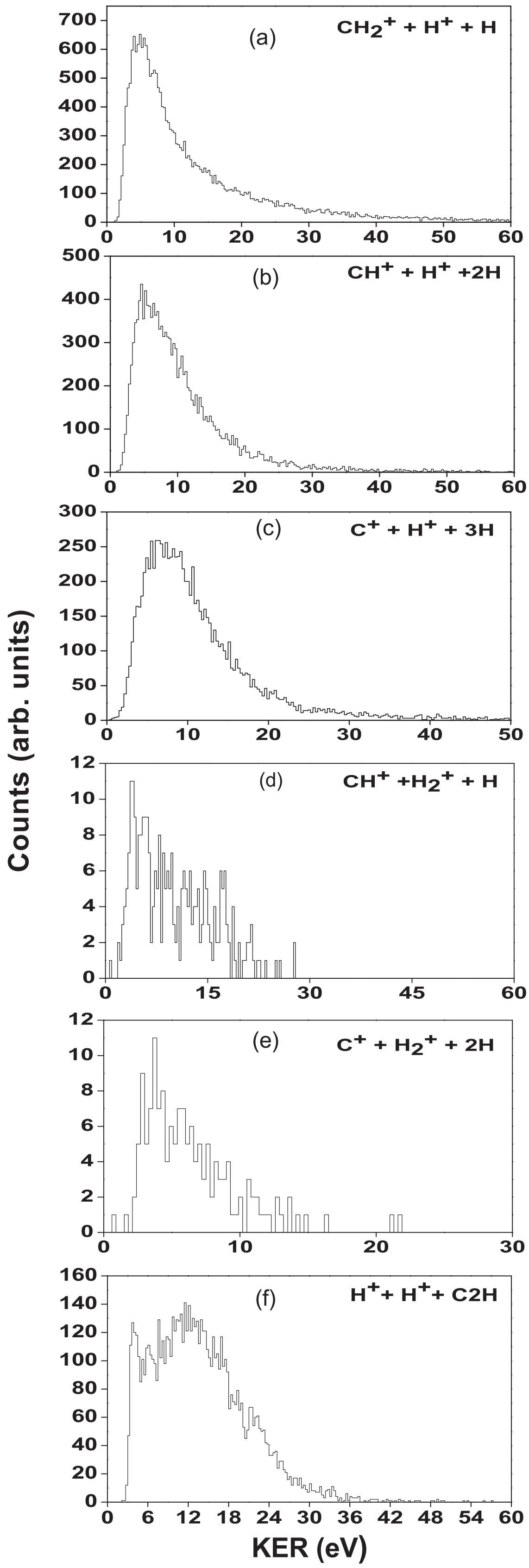

FIG. 4. KER distributions for the incomplete Coulomb explosion channels: (a)–(f) observed in the dissociation of CH_4^{2+} in 10-keV electron impact with CH_4.

electron impact, whereas Ben-Itzhak *et al.* [26] have reported the concerted process for this channel in their experiment.

For the channel $CH^+ + H^+ + 2H$, the slope of the island is -0.90 ± 0.04, which is in reasonable agreement with the theoretically predicted value for the sequential decay process (see Table II). Figure 5(b) shows the Newton diagram for this channel. From this figure, it is found that the CH^+ and H^+ ions are emitted at $152^\circ \pm 15^\circ$ and $112^\circ \pm 15^\circ$ with respect to the momentum vector of H^+ ion plotted on the x axis. It indicates that this process is also a sequential decay where $CH_4{}^{2+}$ dication fragments in the same way as for the above channel, there is only a difference in the second step that $CH_3{}^+$ dissociates into CH^+ and 2H. Ben-Itzhak *et al.* [26] and Flammini *et al.* [28] have reported the similar results from their experiments.

The slope for the channel $C^+ + H^+ + 3H$ is found to be -0.68 ± 0.06, which is slightly higher than the theoretically predicted value for the sequential decay process [s(i)] (see Table II). This suggests that both the sequential and the concerted processes are involved in the fragmentation of this channel. The Newton diagram for this channel is shown in Fig. 5(c). In this diagram, the distributions of the momentum for the C^+ and the 3H are at about $122^\circ \pm 15^\circ$ and $145^\circ \pm 15^\circ$ with respect to the momentum vector of H^+ ion drawn along the x axis. In this case, the C^+ and 3H have broad momentum distributions, which show the possibility that both the sequential and concerted processes are involved in this fragmentation process.

The KERD for the channel $H^+ + H^+ + C2H$ is shown in Fig. 4(f), which peaks at about 11.5 eV $\pm$ 2.0 eV. There are no experimental or theoretical data available in the literature for this channel to compare with. The slope for this channel cannot be determined due to its unclear shape in the ion-ion coincidence map (see Fig. 2). Therefore, we cannot suggest conclusively its dissociation mechanism from the shape and size of the island. The Newton diagram for this channel is shown in Fig. 5(d). In this diagram, the first arriving H^+ ion to the MCP detector is plotted on the x axis and the second arriving H^+ ion to the MCP detector is plotted on the upper half with respect to first arriving H^+ ion. While, the neutral C2H is plotted on the lower half of the x axis with respect to first arriving H^+ ion. It is seen that there are two lobes in the momentum distributions of the second H^+ ion; the lobes have distribution around $116^\circ \pm 20^\circ$ and $160^\circ \pm 20^\circ$. The neutrals C2H have broad distributions around $90^\circ \pm 20^\circ$ and $120^\circ \pm 20^\circ$. These features indicate that there are two fragmentation pathways involved in this channel. In the first case, the second H^+ ion and the neutral C2H are emitted at 116° and 120°, respectively, with respect to the first arriving H^+ ion. This suggests that the fragmentation process is a concerted process and all fragments carry sufficient momenta and they are ejected at large angles to balance the momentum. The similar distributions have been also observed by Williams *et al.* [40] for the collisions of 306-eV photons with CH_4 molecules using cold target recoil ion momentum spectroscopy (COLTRIMS). They have observed the angle between two concomitant H^+ ions larger than the ground-state bond angle of 109.5° and attributed the H^+ ions to eject along the bond axes with broadening of angle due to the Coulomb repulsion of the two H^+ ions. In the second case, second

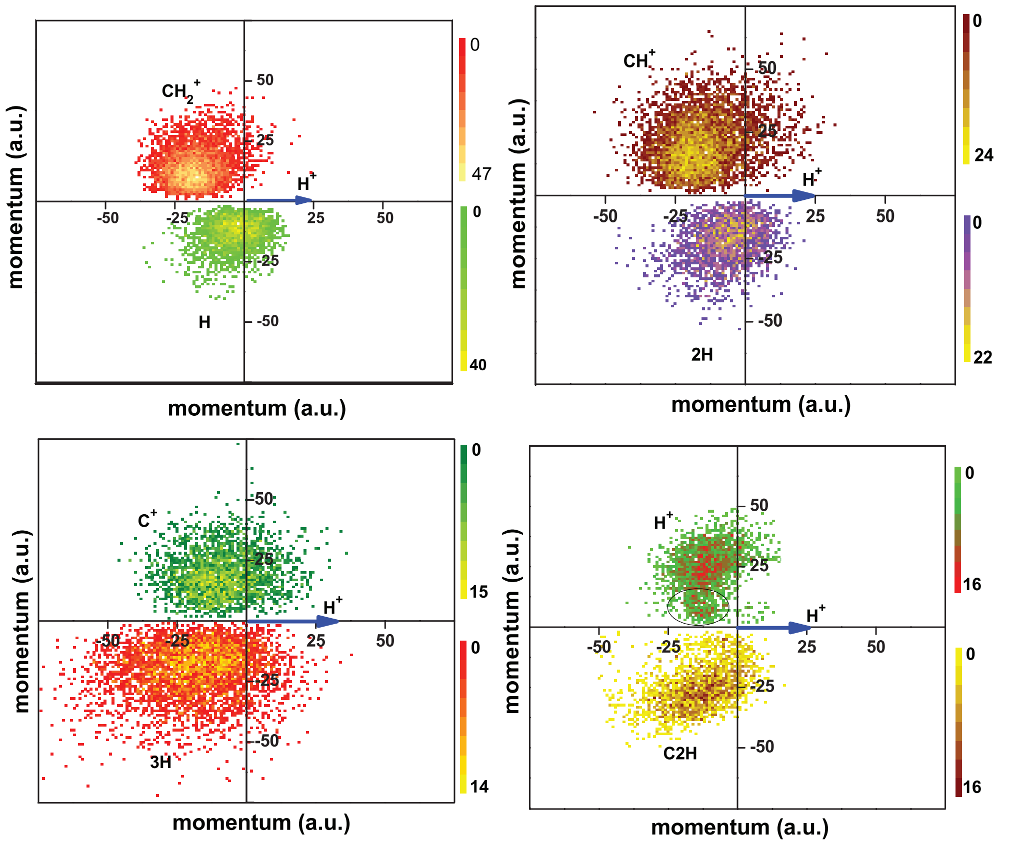

FIG. 5. (Color online) Newton diagrams for the incomplete Coulomb explosion channels: (a) $CH_2^+ + H^+ + H$, (b) $CH^+ + H^+ + 2H$, (c) $C^+ + H^+ + 3H$, and (d) $H^+ + H^+ +$ C2H originating from the dissociation of CH_4^{2+} dication in 10-keV electron impact with CH_4. The momentum vectors of the reference ions are taken along the x axis and the relative momentum vector distributions of the other ions (or neutrals) are plotted in the upper and lower half of the x axis.

arriving H^+ and neutral C2H are ejected at $160^\circ \pm 20^\circ$ and $90^\circ \pm 20^\circ$, respectively, with respect to the first arriving H^+ ion. The momentum distribution for this channel is marked by a circle in Fig. 5(d), which suggests that this fragmentation undergoes a concerted process. But in this process, CH_4^{2+} instantaneously decays into $H^+ + H^+ +$ C2H; both H^+ ions fly almost back-to-back leaving neutral species C2H with a very small momentum around $90^\circ \pm 20^\circ$. The KER for the first case should be large because all fragments carry appreciable momenta while in the second case, the neutral C2H is ejected at $90^\circ \pm 20^\circ$ carrying small momentum. It is also clear from the KERD [see Fig. 4(f)] that there are two distinct peaks situated at around 4.0 eV and 11.5 eV.

The KERDs for the channels $CH^+ + H_2^+ + H$ and $C^+ + H_2^+ + 2H$ are shown in Figs. 4(d) and 4(e), respectively. The peakes of these distributions are found to lie at 4.0 ± 1.0 eV and 3.7 ± 1.0 eV, respectively. Due to unavailability of experimental as well as theoretical KER values in the literature, the comparison could not be made with our data. The statistics for these channels in the ion-ion coincidence map are small. Moreover, we have estimated the slopes for these channels; they are found to be 0.79 ± 0.10 and 0.97 ± 0.10, respectively. The slope for the channel $CH^+ + H_2^+ + H$ is larger than the theoretically predicted value for the sequential decay process [s(i)] (see Table II). The shape of the island is broad, which indicates that the neutral H takes away some momentum from the instantaneous break up of CH_4^{2+} molecular ion. The peak value of the KE distributions for H_2^+, C^+ and H is at 2.5 eV, 0.4 eV and 1.5 eV respectively; this also shows that neutral H gains some finite kinetic energy in this fragmentation channel. Thus, the fragmentation process for this channel is possibly a concerted process. Further, for the channel $C^+ + H_2^+ + 2H$, the slope is very close to -1.0, which suggests that this is a concerted process and the fragment ions fly back-to-back leaving the neutral 2H almost with negligible kinetic energy. This is obvious from the calculated values of kinetic energies of H_2^+, C^+, and 2H, which are 3.3 eV, 0.3 eV, and 0.6 eV, respectively.

IV. CONCLUSION

We have studied the fragmentation dynamics for the CH_4 molecule under impact of 10-keV electrons using the recoil ion momentum spectroscopy. We observe two channels ($CH_3^+ + H^+$, $CH_2^+ + H_2^+$) arising from the complete Coulomb fragmentation and the six channels ($CH_2^+ + H^+ + H$, $CH^+ + H^+ + 2H$, $C^+ + H^+ + 3H$, $H^+ + H^+ +$ C2H, $CH^+ + H_2^+ + H$, and $C^+ + H_2^+ + 2H$) from the incomplete Coulomb fragmentation of CH_4 molecule. The KERD for these channels are determined and compared with those of other workers. It is found that our KERD mostly arises from the lowest electronic states of the $CH_4{}^{2+}$ dication. The dissociation mechanism has been assigned to different dissociation channels arising from the fragmentation of $CH_4{}^{2+}$ dication. It is suggested that for the dissociation channel $H^+ + H^+ + C2H$, the bond mostly breaks along the bond axes of the parent molecule. We also estimate the relative abundance for different ion species arising from the fragmentation of CH_4 with the impact of keV electrons.

ACKNOWLEDGMENTS

The work was supported by the Department of Science and Technology (DST), New Delhi, under the research project: SR/S2/LOP-09/2006. R.S., N.Y., and P.B. thankfully acknowledge the partial supports in form of fellowships by the Council of Scientific and Industrial research (CSIR), New Delhi, and by the Board of Research in Fusion Science & Technology (BRFST), Ahmedabad, during the progress of this work.

[1] D. Mathur, Phys. Rep. **391**, 1 (2004).
[2] S. D. Price, Phys. Chem. Chem. Phys. **5**, 1717 (2003).
[3] J. Rajput and C. P. Safvan, Phys. Rev. A **75**, 062709 (2007).
[4] B. Bapat and V. Sharma, J. Phys. B **40**, 13 (2007).
[5] M. Tarisien *et al.*, J. Phys. B **33**, L11 (2000).
[6] D. Mathur, E. Krishnakumar, K. Nagesha, V. R. Marathe, V. Krishnamurthit, F. A. Rajgara, and U. T. Raheja, J. Phys. B **26**, L141 (1993).
[7] A. Qayyum, W. Schustereder, C. Mair, W. Hess, P. Scheier, and T. D. Mark, Phys. Scr. **T103**, 29 (2003).
[8] B. Boudaiffa, P. Cloutier, D. Hunting, M. A. Huels, and L. Sanche, Science **287**, 1658 (2000).
[9] R. W. Carlson *et al.*, Science **283**, 2062 (1999).
[10] D. E. Shemansky and D. T. Hall, J. Geophys. Res., [Space Phys.] **97**, 4143 (1992).
[11] T. E. Cravens, C. J. Lindgren, and S. A. Levina, Planet. Space Sci. **46**, 1193 (1998).
[12] J. Hunter Waite Jr. *et al.*, Science **311**, 1419 (2006).
[13] http://oceana.org/en/our-work/climate-energy/climate-change/learn-act/greenhouse-gases.
[14] S. H. Lee, J. M. Reeves, J. C. Wilson, D. E. Hunton, A. A. Viggiano, T. M. Miller, J. O. Ballenthin, and L. R. Lait, Science **301**, 1886 (2003).
[15] H. C. Straub, D. Lin, B. G. Lindsay, K. A. Smith, and R. F. Stebbings, J. Chem. Phys. **106**, 4430 (1997).
[16] C. Backx and M. J. Van der Wiel, J. Phys. B **8**, 3020 (1975).
[17] I. Ben-Itzhak, K. D. Carnes, D. T. Johnson, P. J. Norris, and O. L. Weaver, Phys. Rev. A **49**, 881 (1994).
[18] J. H. D. Eland, Chem. Phys. **323**, 391 (2006).
[19] C. Wu, H. Ren, T. Liu, R. Ma, H. Yang, H. Jiang, and Q. Gong, J. Phys. B **35**, 2575 (2002).
[20] P. M. Sieghbahn, Chem. Phys. **66**, 443 (1982).
[21] G. Dujardin, D. Winkoun, and S. Leach, Phys. Rev. A **31**, 3027 (1985).
[22] D. A. Erwin and J. A. Kunc, Phys. Rev. A **72**, 052719 (2005).
[23] R. Singh, P. Bhatt, N. Yadav, and R. Shanker, Meas. Sci. Technol. **22**, 055901 (2011).
[24] Beckord, U. Werner, and H. O. Lutz, Nucl. Instrum. Methods A **337**, 409 (1994).
[25] J. Ullrich, R. Moshammer, A. Dorn, R. Dörner, L. Ph. H. Schmidt, and H. Schmidt-Böcking, Rep. Prog. Phys. **66**, 1463 (2003).
[26] I. Ben-Itzhak, K. D. Carnes, S. G. Ginther, D. T. Johnson, P. J. Norris, and O. L. Weaver, Phys. Rev. A **47**, 3748 (1993).
[27] B. Siegmann, U. Werner, and R. Mann, Nucl. Instrum. Methods B **233**, 182 (2005).
[28] R. Flammini, M. Satta, E. Fainelli, G. Alberti, F. Maracci, and L. Avaldi, New J. Phys. **11**, 083006 (2009).
[29] E. Kukk *et al.*, J. Phys. B **40**, 3677 (2007).
[30] P. Bhatt, R. Singh, N. Yadav, and R. Shanker, Phys. Rev. A **84**, 042701 (2011).
[31] I. H. Wiley and W. C. McLaren, Rev. Sci. Instrum. **26** 1150 (1955).
[32] http://www.roentdek.com/.
[33] P. Bhatt, R. Singh, N. Yadav, and R. Shanker, Phys. Rev. A **82**, 044702 (2010).
[34] J. H. D. Eland, Mol. Phys. **61**, 725 (1987).
[35] J. H. D. Eland, Laser Chem. **11**, 259 (1991).
[36] P. Bhatt, R. Singh, N. Yadav, and R. Shanker, Phys. Rev. A **85**, 042707 (2012).
[37] R. K. Janev and D. Reiter, Phys. Plasmas **11**, 780 (2004).
[38] B. Adamczyk, A. J. H. Boerboom, B. L. Schram, and J. Kistemaker, J. Chem. Phys. **44**, 4640 (1966).
[39] S. W. J. Scully, J. A. Wyer, V. Senthil, and M. B. Shah, J. Electron Spectrosc. Relat. Phenom. **155**, 81 (2007).
[40] J. B. Williams *et al.*, J. Phys. B **45**, 194003 (2012).
[41] D. L. Hansen *et al.*, J. Phys. B **32** 2629 (1999).
[42] S. Wexler, J. Chem. Phys. **41**, 2781 (1964).